NATIONAL ADVISORY COMMITTEE FOR AERONAUTICS

TECHNICAL NOTE 2723

USE OF THE BOUNDARY LAYER OF A CONE TO MEASURE SUPERSONIC FLOW INCLINATION

By Franklin K. Moore

Lewis Flight Propulsion Laboratory
Cleveland, Ohio

NACA
Washington
June 1952

NATIONAL ADVISORY COMMITTEE FOR AERONAUTICS

TECHNICAL NOTE 2723

USE OF THE BOUNDARY LAYER OF A CONE TO MEASURE SUPERSONIC FLOW INCLINATION

By Franklin K. Moore

SUMMARY

An instrument is suggested for the measurement of supersonic flow inclination, taking advantage of the effect of angle of attack on the meridional velocity profile of the laminar boundary layer on a cone. This effect of angle of attack may be measured by the difference of total pressure recorded by two probes pointing toward the apex and located in the plane of symmetry of the flow.

The theoretical response to angle of attack is derived and found to depend essentially on the ratio of angle of attack to cone semivertex angle. Thus, the more slender the cone, the greater the sensitivity to angle of attack, subject to restrictions imposed by the displacement effect of the boundary layer.

Results of a single test are presented and discussed. The results show that sensitivity is limited to angles of attack less than the cone semivertex angle. The effect of probe size is discussed.

Equations are presented which permit the probes to be located in such a way that maximum sensitivity is obtained. A method is described whereby the instrument may be calibrated for zero flow inclination.

INTRODUCTION

In reference 1, an analysis of the laminar boundary layer on a circular cone in supersonic flow showed that the effect of a small change in angle of attack on the boundary-layer velocity profile in the plane of symmetry is proportionately quite large. Figure 1 shows the notation and terminology used in this report.

A positive angle of attack induces a secondary flow of low-energy air from beneath the cone toward the top, with the consequence that the meridional skin friction is lower on the top of the cone than on the

bottom, whereas the thickness of the boundary layer is greater on the top than on the bottom. For example, the variation with angle of attack of the laminar skin friction on the top side of the cone in the plane of symmetry is predicted to be as shown in figure 2. The data for $\Theta = 10$, 20, and 30 are given in reference 1 and the curve for $\Theta = 0$ is based on the boundary-layer theory of reference 1 but embodies the use of linearized potential theory for the outer nonviscous flow. Figure 2 shows that an angle of attack α, which is a certain fraction α' of the cone semivertex angle Θ, will cause a fractional change of the same order as α' in the meridional skin friction.

From this result, measurements of the velocity profile in the meridional planes of a cone in supersonic flow evidently would provide sensitive indication of the angularity of the incident flow with respect to the cone axis. The proportional sensitivity of an instrument to perform such measurements would depend chiefly on the slenderness of the cone used. Thus the more sensitive the configuration, the less bulky it would be and, hence, the more easily adapted to detailed surveys of flow angularity.

The theoretical performance of a flow-angularity indicator utilizing the changes due to angle of attack in the meridional laminar velocity profile is discussed herein, and limited experimental results are described. This research was conducted at the NACA Lewis laboratory.

DESCRIPTION OF INSTRUMENT

The circular cone must be fitted with fixed instrumentation for sensing changes due to angle of attack in the meridional velocity profile. Many methods might be devised to perform this function. The particular technique contemplated in this report is the following: Two fixed total-head probes are mounted in a meridional plane, the tips of the probes pointing toward the cone apex and located at a height above the cone surface so as to be well inside the boundary layer (fig. 1). The difference between the total pressures measured by these two probes would indicate the angle of attack in the meridional plane.

In order to avoid extensive calibration, null operation is desirable for many applications, especially if the angle of attack and yaw are both to be determined. For this purpose, four probes could be used, equally spaced around the cone and at the same height above the surface. The total pressure measured by each opposing pair could then be balanced by a null procedure.

The location of a pair of probe tips relative to the cone surface may be obtained from equations developed as follows: For a given Mach

number and cone angle, the response of the instrument (to be discussed in the following section) depends on the height of the effective centers of the probe apertures above the surface, expressed as the dimensionless coordinate λ, defined in reference 1 as

$$\lambda = \sqrt{\frac{3C\bar{\mu}}{\bar{\rho}ux}} \sqrt{\frac{\bar{p}}{p}} \int_0^{\overline{\rho u}y/C\bar{\mu}} \frac{\rho}{\bar{\rho}} d(\overline{\rho u}y/C\bar{\mu}) \tag{1}$$

The symbols ρ, u, μ, and p represent the density, meridional velocity component, coefficient of viscosity, and pressure in the boundary layer, respectively; the bars above these quantities signify evaluation at the outer edge of the cone boundary layer for zero angle of attack, or, alternatively, surface values of the nonviscous flow tabulated in reference 2. The surface velocity is given in references 2 and 3 as a dimensionless quantity, designated in this report as $\bar{u}_s$ (in references 2 and 3, as $\bar{u}$ and $\bar{u}_s$, respectively), which is related to the actual velocity $\bar{u}$ as follows

$$\bar{u} = \bar{u}_s\sqrt{7RT_t} \tag{2}$$

where T_t is the total temperature. A complete list of symbols is given in the appendix. Equation (1) incorporates the compressibility correction of Howarth (reference 4), the assumption of the relation

$$\frac{\mu}{\bar{\mu}} = C\frac{T}{\bar{T}} \tag{3}$$

between temperature and viscosity in the boundary layer (reference 5), and a statement of similarity of the boundary-layer flow in meridional planes; that is, in a meridional plane

$$\frac{u}{\bar{u}}(x,y) = \frac{u}{\bar{u}}(\lambda)$$

At zero angle of attack,

$$\frac{u}{\bar{u}} = \frac{d}{d\lambda} f_0(\lambda)$$

which is the dimensionless velocity distribution of Blasius.

Under the assumptions of Prandtl number equal to 1 and zero heat transfer through the cone surface, the energy equation yields, for $\alpha = 0$ (reference 1),

$$\frac{\overline{\rho}}{\rho} = 1 + \frac{M^2}{5}\left[1 - \left(\frac{df_0}{d\lambda}\right)^2\right] \tag{4}$$

where the ratio of specific heats is 1.4. Equation (1) may be inverted to yield, for $\alpha = 0$,

$$\frac{\overline{\rho u}y}{C\overline{\mu}} = \sqrt{\frac{\overline{\rho u}x}{3C\overline{\mu}}}\int_0^{\lambda} \frac{\overline{\rho}}{\rho}\, d\lambda \tag{5}$$

Equations (4) and (5) indicate that λ is constant along parabolas from the cone apex. As will be shown subsequently, for $M_0 \approx 3$ and in the limit of vanishing Θ, maximum sensitivity is obtained for $\lambda = 3.6$. For this value of λ, equations (4) and (5) yield the particular parabola

$$\frac{\overline{\rho u}y}{C\overline{\mu}} = \sqrt{\frac{\overline{\rho u}x}{3C\overline{\mu}}}\left(3.600 + 2.322\,\frac{\overline{M}^2}{5}\right) \tag{6}$$

The quantity C is obtained by matching equation (3) to the Sutherland formula at the cone surface, as recommended in reference 5. The result is

$$C = \frac{T_t\,(1 - u_s^2) + 216^\circ\ R}{(T_t + 216^\circ\ R)\sqrt{1 - \overline{u}_s^2}} \tag{7}$$

Thus, in order for the effective center of the probe tip to be located at a predetermined value of λ (selected to provide maximum sensitivity), the probe may be placed anywhere along the parabola given by equation (5). Of course, if any significant streamwise variation of flow inclination is anticipated, the probe tips should be placed as close as possible to the cone apex.

For the test to be described later in this report, a cone with a semivertex angle of 7.5° was used. The two total-head probes were made of 0.015-inch outside diameter stainless-steel tubing, flattened to give an aperture height of 0.005 inch. Both apertures were placed 2 inches aft of the cone apex. The geometrical center of one probe

was 0.012 inch above the surface and the other 0.014 inch. (The difference was due to inaccuracy of fabrication.) For the conditions of the test (Mach number, 3.1; total temperature, 200° F; and total pressure equal to atmospheric) these probe locations correspond to $\lambda = 2.6$ and 3.0, respectively, assuming that the effective centers of the probes are equal to the geometrical center.

THEORETICAL AND EXPERIMENTAL PERFORMANCE

Theoretical Response Derivative

The basic response characteristic of the proposed instrument is

$$-\left[2\partial(H/p_0)/\partial\alpha\right]_{\alpha=0}$$

where H/p_0 is the ratio of total pressure measured in, for example, the top tube to the static pressure ahead of the cone. The factor of 2 is required in order to account for the fact that differences in total pressure are to be measured.

From the analysis of reference 1, for a small positive angle of attack, the relation

$$\frac{u}{\bar{u}} = \frac{d}{d\lambda} f_0(\lambda) + \alpha A_1 \frac{d}{d\lambda} f_1(\lambda)$$

applies in the boundary layer in the plane of symmetry at the top of the cone. The quantity A_1 is obtained from reference 3 and $f_0(\lambda)$ and $f_1(\lambda)$ are obtained from reference 1. Thus,

$$\left(\frac{\partial u/\bar{u}}{\partial\alpha}\right)_{\alpha=0} = \left(\frac{\partial\lambda}{\partial\alpha}\right)_{\alpha=0} \frac{d^2}{d\lambda^2} f_0(\lambda) + A_1 \frac{d}{d\lambda} f_1(\lambda) \tag{8}$$

From the definition of λ in reference 1, the value of $(\partial\lambda/\partial\alpha)_{\alpha=0}$ may be obtained. Assuming T_t constant through the boundary layer (that is, Pr = 1 and zero heat transfer, for this case) and using the relation

$$\bar{M}^2 = 5 \frac{\bar{u}_s^2}{1 - \bar{u}_s^2}$$

result in the following relation between velocity and Mach number profiles in the boundary layer:

$$\frac{u}{\bar{u}} = \frac{1}{\bar{u}_s} \frac{M}{\sqrt{5+M^2}} \tag{9}$$

If $M > 1$, the normal shock relations (see reference 6) provide that the observed total pressure is

$$\frac{H}{p} = \left(\frac{6}{5} M^2\right)^{7/2} \left(\frac{7M^2 - 1}{6}\right)^{-5/2} \tag{10a}$$

or, if $M < 1$, isentropic flow relations yield

$$\frac{H}{p} = \left(\frac{5 + M^2}{5}\right)^{7/2} \tag{10b}$$

Further,

$$\left[\frac{\partial}{\partial\alpha} (H/p_0)\right]_{\alpha=0} = \frac{\bar{p}}{p_0} \left[\frac{H}{p} \frac{\partial}{\partial\alpha} (p/\bar{p}) + \frac{\partial}{\partial\alpha} (H/p)\right]_{\alpha=0} \tag{11}$$

and, at the top of the cone, in the notation of reference 1,

$$\frac{p}{\bar{p}} = 1 - \alpha A_3 \tag{12}$$

Equations (8) to (12) may be used to evaluate the required response $-\left[2\partial(H/p_0)/\partial\alpha\right]_{\alpha=0}$ for a given value of λ, in terms of the basic parameters of the flow. With the use of the definition

$$\alpha' \equiv \alpha/\Theta$$

the result may be obtained in the form

$$-2\left[\frac{\partial}{\partial\alpha'} (H/p_0)\right]_{\alpha=0} = 2\Theta \frac{\bar{p}}{p_0} \sum_{n=1}^{4} G_n(M_0,\Theta,\lambda)\, A_n \tag{13}$$

where the G_n are functions which may be tabulated as follows for $\lambda = 3.6$:

2485

$\bar{u}_s$	G_1	$G_2 \sin \Theta$	G_3	G_4
0.4	-2.068	0.3783	1.369	0.6872
.5	-4.406	.9801	1.711	1.505
.6	-7.944	2.215	2.455	2.840
.7	-13.56	5.429	4.085	5.272
.8	-21.68	16.93	8.874	10.28
.9	-15.16	95.01	33.32	21.64

In terms of the notation used in reference 3,

$$\left.\begin{aligned} A_1 &= -x/\bar{u}_s \\ A_2 &= -z/\bar{u}_s - 2x/(\bar{u}_s \sin \Theta) \\ A_3 &= \eta/\bar{\rho} \\ A_4 &= \xi/\bar{\rho} \end{aligned}\right\} \tag{14}$$

The quantity $\bar{p}/p_0$ is tabulated in reference 2 (where the equivalent notation is p_s/p_0).

The smallest semivertex angle Θ for which tabulations are made in reference 3 is 5°. By linearized potential theory (still with the assumption, as in references 1 and 3, that $\alpha \ll \Theta$)

$$\left.\begin{aligned} A_2 &= 2 \\ \bar{M}/M_0 &\approx \bar{p}/p_0 \approx 1 \end{aligned}\right\} \tag{15}$$

Clearly, in the limit of vanishing Θ, only the second term of equation (13) need be retained.

The response $-\left[2\partial(H/p_0)/\partial\alpha'\right]_{\alpha=0}$ is shown in figure 3, as computed from equation (13) and the accompanying table. The values of M_0 corresponding to various values of $\bar{u}_s$ and Θ may be found in references 2 or 3. The curve for $\Theta = 15^\circ$ is essentially identical to the limiting curve for $\Theta = 0$, obtained by use of equations (13) and (14), and therefore the figure shows that this instrument may be expected to respond essentially to $\alpha' = \alpha/\Theta$ rather than to α itself.

Supersonic flow inclination may be measured by the difference in static pressure on the two faces of a wedge. The static-pressure response $-\left[2\partial(p/p_0)/\partial\alpha'\right]_{\alpha=0}$ for such a wedge with a half-angle of 10° as obtained by shock-wave theory is shown in figure 3.

Given M_0 and Θ, λ may be varied in order to determine from equation (13) the λ for which $-\left[2\partial(H/p_0)/\partial\alpha'\right]_{\alpha=0}$ is a maximum. The variation of the response with λ for $M_0 = 2.98$ and $\Theta = 0$ is shown in figure 4. Under these conditions the maximum response is to be expected when the probe-tip location corresponds to $\lambda = 3.6$. When $M_0 = 1.91$ and $\Theta = 0$, a maximum response of 14.4 is obtained for $\lambda = 3.3$, as compared with a response of 13.6 for $\lambda = 3.6$; and when $M_0 = 3.94$ and $\Theta = 0$, the maximum response is 218 for $\lambda = 3.9$, while the response for $\lambda = 3.6$ is 202. Therefore, the use of the value $\lambda = 3.6$ for placing the probes (equation (6)) will yield a response close to the maximum over a range of Mach number between 2 and 4. This result presumably applies reasonably well over a range of cone angle, inasmuch as figure 3 shows that the response in terms of α' depends only slightly on Θ.

2485

Experimental Results and Discussion

The circled point on figure 3 represents the result of a test made under the conditions previously described. Also shown is a segment of the corresponding theoretical curve for $\lambda = 2.8$, which is the average theoretical value of λ for the two tubes, assuming effective and geometrical centers to be the same. Figure 5 shows the ratio of the total pressure measured in each probe to stream static pressure, as the angle of attack was varied. Also shown is a curve of the ratio of the difference between the total pressures measured in the two probes to stream static pressure, at each angle of attack. The latter curve represents the use of the instrument for the indication of angle of attack, and the slope of this curve at zero angle of attack provides the experimental point of figure 3.

Effect of boundary-layer displacement. - The experimental configuration did not achieve the expected theoretical response. The discrepancy is due, at least in large part, to the displacement effect of the boundary layer on the outer flow. This effect will manifest itself in two ways:

(1) Because of the displacement thickness, the cone has an effective vertex angle larger than the geometrical constructed angle. Under the conditions of the test, the displacement thickness 2 inches aft of

apex is about 0.012 inch at zero angle of attack (see reference 1). Therefore, there is, in effect, an increment in semivertex angle of the order of 0.006 radian, or about 5 percent of the total semivertex angle. Thus, near zero angle of attack, the scale of α' in figure 5 should be linearly expanded by approximately 5 percent. Relative to this scale of effective α', the slope of the experimental response curve is greater than that relative to the geometrical scale.

(2) For a small positive angle of attack, the displacement thickness on top of the body is greater, and on the bottom less, than at zero angle of attack. Thus the effective angle of attack is less than the geometrical angle of attack. In reference 7 the actual displacement thickness in the plane of symmetry at the top of the cone is shown to be

$$\Delta = \delta_x + \frac{2}{3} \frac{\alpha}{\sin \Theta} (\delta_x - \delta_\varphi) A_2$$

where values of δ_x and δ_φ may be obtained from reference 1. Under the conditions of the test, at a distance 2 inches aft of the apex, the increment in displacement thickness due to angle of attack is about 0.16 inch per radian, or the effective decrement in angle of attack is about 0.08 radian per unit angle of attack in radians. Thus, near zero angle of attack, the scale of α' in figure 5 should be expanded by about 8 percent to account for this effect.

Accordingly, relative to a scale of effective α', the experimental response is of the order of 13 percent higher than the response measured directly. This correction applied to the experimental point of figure 3 would account for about half of the discrepancy between theory and experiment. This estimate should be regarded as correct only as to order of magnitude because, although the effect of the theoretical boundary layer on the outer flow can be determined approximately, at the present time no proper basis for revising the boundary-layer solution in accord with the corrected outer flow exists.

The effect of boundary-layer displacement limits the sensitivity of the instrument. That is, if Θ is decreased, the sensitivity would be increased proportionally provided the boundary layer remains infinitesimally thin compared with the cone. However, as Θ is decreased, the deleterious effects of displacement are proportionally greater and, for a sufficiently small Θ, will predominate over the theoretical effects neglecting displacement. This limitation is of course more serious for low Reynolds numbers.

Effect of probe size. - The aperture of the probe used in the test (0.005 in.) is a considerable portion of the boundary-layer thickness

(about 0.025 in.). Thus, the effect of probe size might be expected to contribute to the discrepancy between theory and experiment.

Unpublished data obtained by Robert E. Blue of the Lewis laboratory indicate that in the boundary layer of a flat plate in supersonic flow a large-aperture probe will measure a lower total pressure in the supersonic portion of the boundary layer than will a small-aperture probe, if the two probe centers are at the same height above the plate. Therefore, the present measurements will be affected in two ways:

(1) The effective center of the probe will be closer to the cone surface than will be the geometrical center and, hence the probe will respond at a lower value of y (or λ) than that value of y appropriate to the geometrical center. This means lower sensitivity to angle of attack (see fig. 4) and the effect is in the proper direction to contribute to an explanation of the discrepancy between theory and experiment. Of course, in practice, the probe location may be adjusted to place the effective probe center at the design value of λ.

(2) Probably, the effect of probe size varies directly with the gradient of total pressure in which the probe tip is immersed. From figure 4, it may be seen that for the conditions of the test ($\lambda = 2.8$)

$$-\frac{\partial}{\partial\lambda}\left[2\,\frac{\partial(H/p_0)}{\partial\alpha'}\right]_{\alpha=0} > 0$$

or

$$\frac{\partial}{\partial y}\left[2\,\frac{\partial(H/p_0)}{\partial\alpha'}\right]_{\alpha=0} = 2\left[\frac{\partial}{\partial\alpha'}\,\frac{\partial(H/p_0)}{\partial y}\right]_{\alpha=0} < 0$$

This means that the total-head gradient in which the top probe is immersed decreases as the angle of attack is increased. Thus, it is expected that in going from a negative to a positive value of the angle of attack, there is a decrease in the amount by which the top probe reads too low. Figure 5 shows that this effect is equivalent to a decrease in sensitivity and, hence, contributes to an explanation of the discrepancy between theory and experiment. It seems likely that this effect may be avoided by operation at values of λ equal to or greater than that for peak sensitivity ($\lambda = 3.6$, fig. 4) for which

$$\left[\frac{\partial}{\partial\alpha'}\,\frac{\partial(H/p_0)}{\partial y}\right]_{\alpha=0} = 0$$

High angle-of-attack effects. - According to figure 5, the total pressure measured by the top probe decreases as the angle of attack increases from zero. This signifies, of course, that the meridional skin friction is decreasing, as would be expected from secondary flow considerations. However, at an angle of attack of about 6° this trend reverses, and the meridional skin friction apparently begins to increase as the angle of attack is increased further. On the basis of theoretical work not yet completed, this behavior is probably characteristic of the laminar boundary layer and is not, for example, connected with transition. The reversal probably depends most on $\alpha' = \alpha/\Theta$, especially for small values of Θ, and occurs in the present case at $\alpha' = 1$.

This aspect of the experimental result indicates that, in general, $2\partial(H/p_0)/\partial\alpha' = 0$ for some value of α' of the order of 1. Accordingly, the usefulness of this instrument for measurement of angle of attack is restricted to a range of angle of attack for which $\alpha' < 1$. Thus, the more slender the cone, the narrower the range of angle of attack that can be measured. This is the disadvantage of using more slender cones in order to obtain the greater sensitivity to small angles of attack which has been discussed previously.

Errors in Locating Probes

The following practical difficulties are likely to arise in the installation of the probes at the design position above the cone surface:

(1) The effective centers of the probe apertures may not be at the same height above the cone surface. Balanced total-pressure measurements of the top and bottom probes will then not correspond to zero angle of attack. If the probes are nearly, but perhaps not precisely, at the same height above the surface, the following calibration procedure might be used to establish the true angle of attack corresponding to balanced pressure readings:

(a) Establish the null point of the instrument, and record the pressure measured by one of the probes.

(b) Rotate the cone 180° about its axis and record the pressure measured by the same probe. If the two measured pressures are different, then the null point clearly does not correspond to zero flow inclination. For example, if, at the null point, the top probe reads higher when rotated 180° from its original position, then the top probe is farther from the surface than is the bottom probe, and the null point corresponds to a positive angle of attack.

(c) Repeat these measurements with the same probe at a slightly different inclination (slightly lower angle of attack for the example just cited).

(d) Thus, as shown in the following sketch, two points are established on each of a pair of curves of the type in figure 5 for the individual probes, except that both curves now correspond to precisely the same height, since the same probe has been used for each. Straight lines may now be passed through these two pairs of points (see sketch) and the intersection provides the cone inclination which corresponds to zero angle of attack.

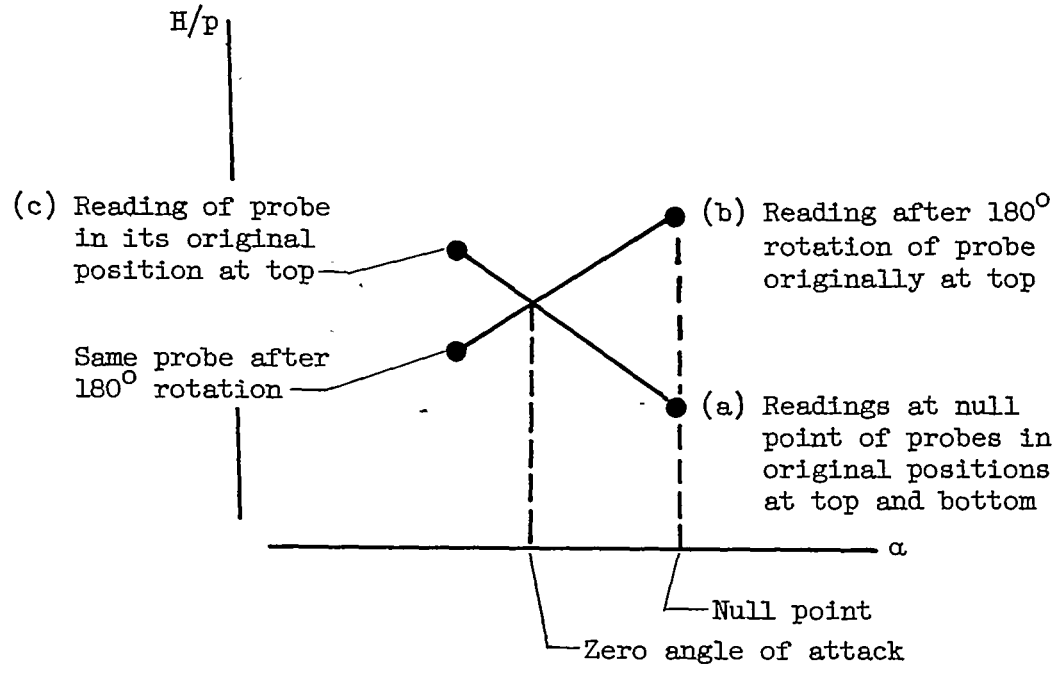

2485

Once the relation between the null inclination and the inclination for zero angle of attack is known, then the instrument may be used without alteration. For the experimental results presented herein, the heights of the two probes were measured and were found to be 0.012 and 0.014 inch. From this information, the expected difference in total pressure measured by the two probes at zero angle of attack was computed. The cone setting corresponding to this observed difference was taken as the origin of the scale of α' in figure 5. This procedure, of course, involves uncertainties and is not recommended for general use.

(2) The probes may not be at the average height corresponding to $\lambda = 3.6$, and, thus, sensitivity is impaired. Figure 6 shows the total pressure that a probe located at a height corresponding to $\lambda = 3.6$ would be expected to record at zero angle of attack. These curves might be used to adjust the average effective height to $\lambda = 3.6$.

CONCLUSIONS

The effect of angle of attack on the meridional velocity profile in the boundary layer of a cone in supersonic flow may be used in an instrument to measure flow angularity. The instrument considered herein consists of a pair of total-head probes lying in the meridional plane in which angle of attack is to be measured. The difference in total pressure recorded by these tubes constitutes an indication of angle of attack. Two pairs of probes might be used to provide simultaneous indication of angle of attack and yaw.

In laminar flow, the response is constant for probe-tip locations along any parabola from the cone apex. A particular parabola, along which the response is a maximum, may be selected for any Mach number and cone angle.

The response at zero angle of attack depends chiefly on Mach number and on the ratio between angle of attack and cone semivertex angle. Theoretically, then, the instrument may be made arbitrarily sensitive to angle of attack, depending on the slenderness of the cone. In practice, a limitation is imposed by the boundary-layer displacement effect, which results in an increase in effective cone angle and a decrease in effective angle of attack.

Results of a single test at $M_0 = 3.1$ and $\Theta = 7.5^\circ$ are presented. The results show that sensitivity to angle of attack exists only for angles of attack less than the semivertex angle of the cone. A rather large discrepancy exists between theoretical response and this particular experiment, and this discrepancy probably is due to a combination of the effects of displacement thickness and height of probe aperture. It is expected that the latter effect may be avoided by operation at the λ for maximum response.

With the use of usual methods of fabrication, discrepancy in probe location above the surface will occur. The true cone setting for zero flow inclination may, however, be determined by a calibration procedure involving a 180° rotation of the cone about its axis.

Lewis Flight Propulsion Laboratory
National Advisory Committee for Aeronautics
Cleveland, Ohio, February 12, 1952

APPENDIX - SYMBOLS

The following symbols are used in this report:

A_1, A_2, A_3, A_4	quantities related to outer nonviscous flow (see equations (14) of this report and reference 1)
C	function of T_t and $\bar{u}_s$ (equation (7)) arising from assumption of linear temperature-viscosity relation
C_{f_x}	local meridional laminar skin-friction coefficient
f_0, f_1	velocity profile functions tabulated in reference 1
G_1, G_2, G_3, G_4	functions of M_0, Θ, and λ (equation (13))
H	total pressure recorded by total-head probe
M	Mach number
Pr	Prandtl number
p	static pressure
R	gas constant
T	static temperature
T_t	total temperature
u	velocity in the x-direction (fig. 1)
$\bar{u}_s$	dimensionless velocity defined in references 2 and 5 (see equation (2))
x	distance from apex of cone to aperture of total-head probe (fig. 1)
y	distance from surface of cone to center of probe aperture (fig. 1)
α	angle of attack of cone, positive in sense shown in figure 1
α'	ratio of angle of attack to cone semivertex angle, α/Θ
Δ	displacement thickness

δ_x, δ_φ	quantities defined in reference 1
Θ	cone semivertex angle
λ	dimensionless coordinate constant along parabolas from cone apex (see equation (1) of this report and reference 1)
μ	coefficient of viscosity
ρ	density

The subscript 0 refers to conditions ahead of the cone.

A bar over a quantity (as in $\bar{\rho}$) refers to evaluation of the nonviscous outer flow at the surface of the cone for zero angle of attack.

REFERENCES

1. Moore, Franklin K.: Laminar Boundary Layer on a Circular Cone in Supersonic Flow at a Small Angle of Attack. NACA TN 2521, 1951.

2. Anon.: Tables of Supersonic Flow Around Cones. Tech. Rep. No. 1, Dept. Elec. Eng., M.I.T., 1947.

3. Anon.: Tables of Supersonic Flow Around Yawing Cones. Tech. Rep. No. 3, Dept. Elec. Eng., M.I.T., 1947.

4. Howarth, L.: Concerning the Effect of Compressibility on Laminar Boundary Layers and Their Separation. Proc. Roy. Soc. (London), ser. A, vol. 194, no. A1036, July 28, 1948, pp. 16-42.

5. Chapman, Dean R., and Rubesin, Morris W.: Temperature and Velocity Profiles in the Compressible Laminar Boundary Layer with Arbitrary Distribution of Surface Temperature. Jour. Aero. Sci., vol. 16, no. 9, Sept. 1949, pp. 547-565.

6. The Staff of the Ames 1- by 3-Foot Supersonic Wind-Tunnel Section: Notes and Tables for Use in the Analysis of Supersonic Flow. NACA TN 1428, 1947.

7. Moore, Franklin K.: The Displacement Thickness of Three-Dimensional Boundary-Layer Flow. NACA TN 2722, 1952.

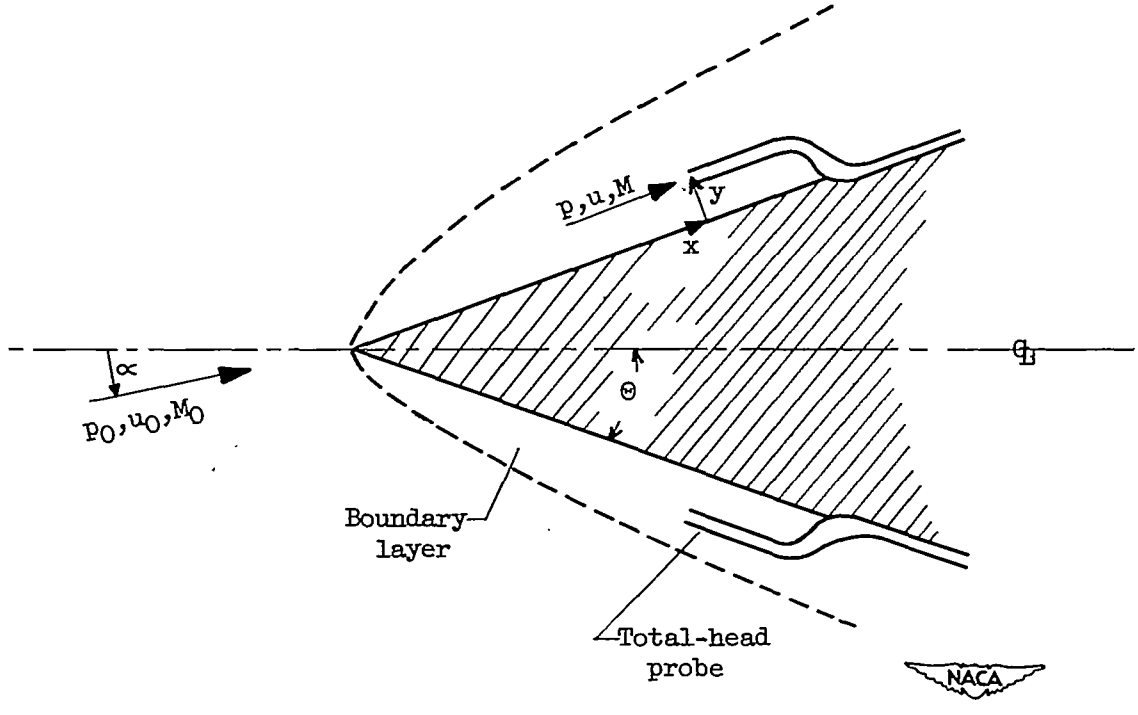

Figure 1. - View of cone in plane of symmetry of flow.

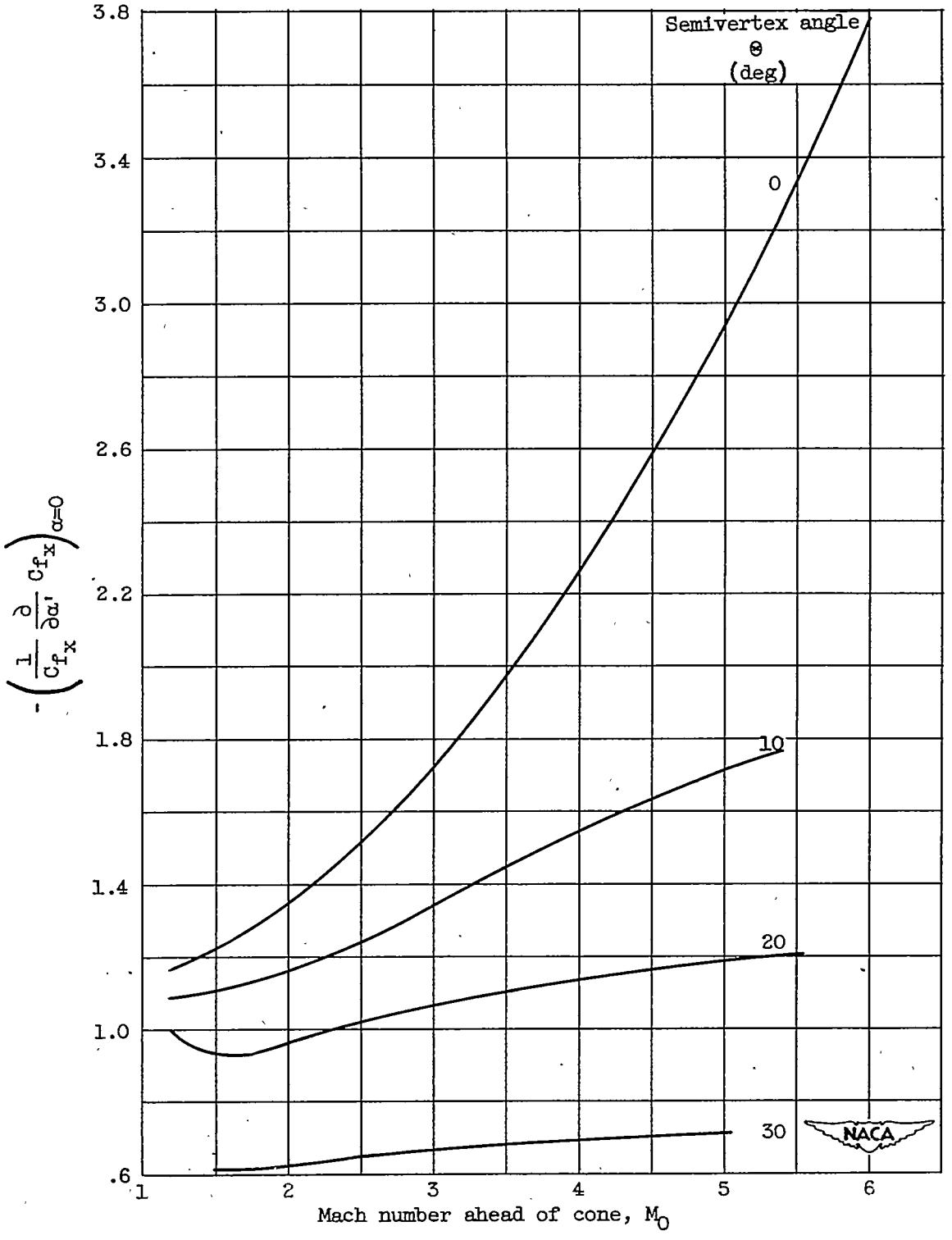

Figure 2. - Increment in skin friction due to angle of attack, in plane of symmetry, at top of cone.

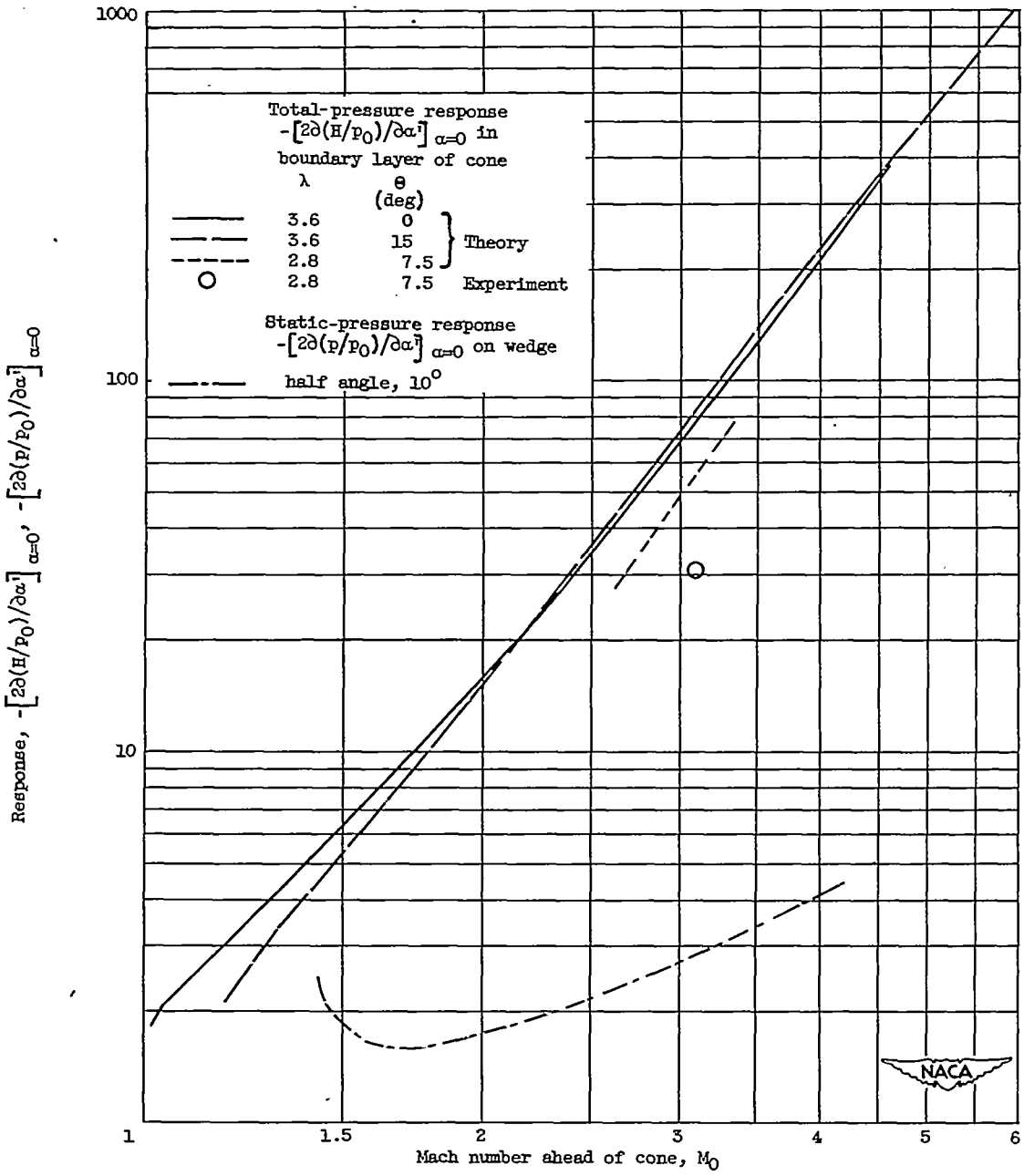

Figure 3. - Response to angle of attack.

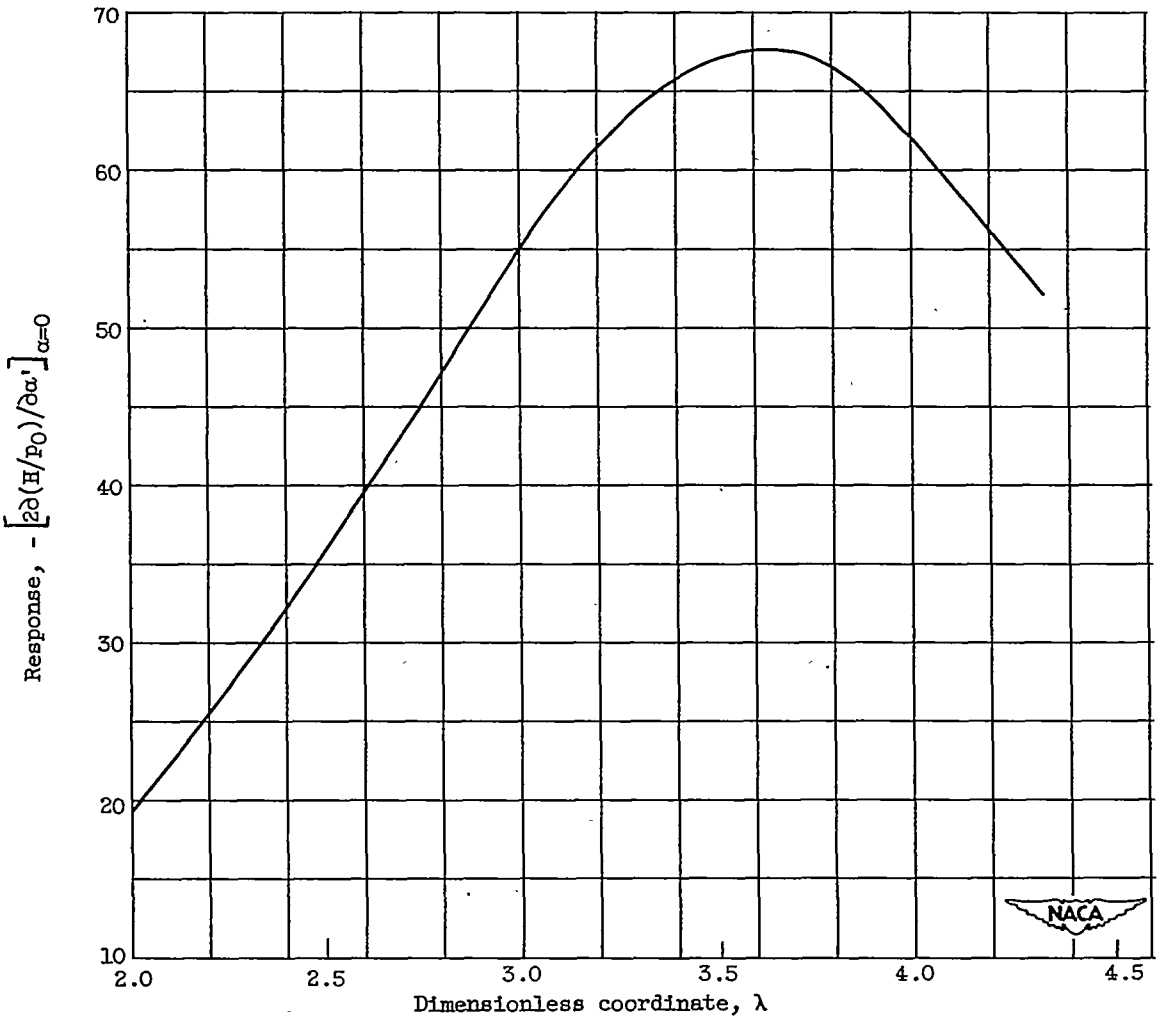

Figure 4. - Variation of response with λ. Mach number ahead of cone, M_0, 2.98; cone semivertex angle, θ, 0.

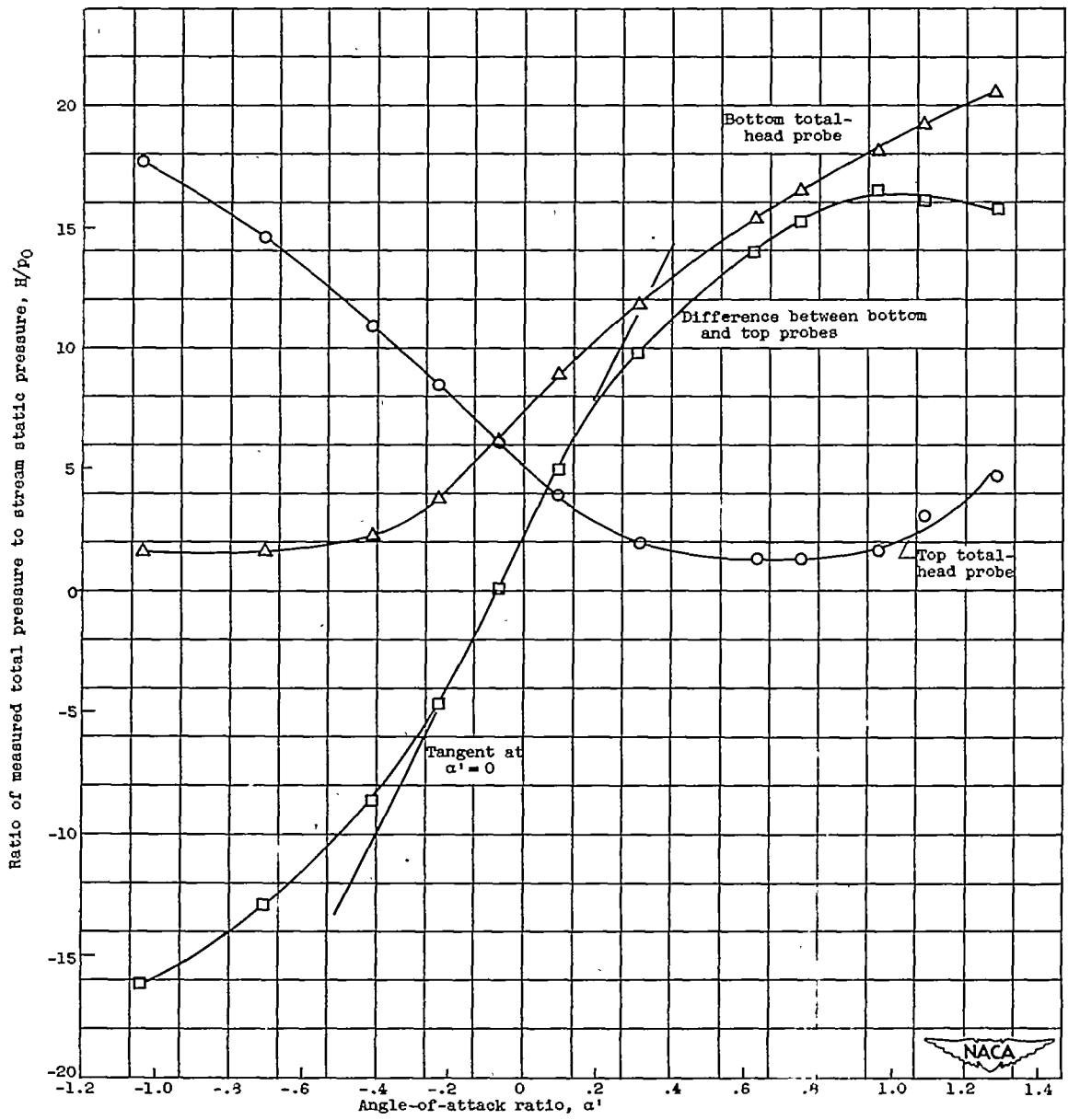

Figure 5. - Experimental performance, Mach number ahead of cone, M_0, 3.1; cone semivertex angle, θ, 7.5°.

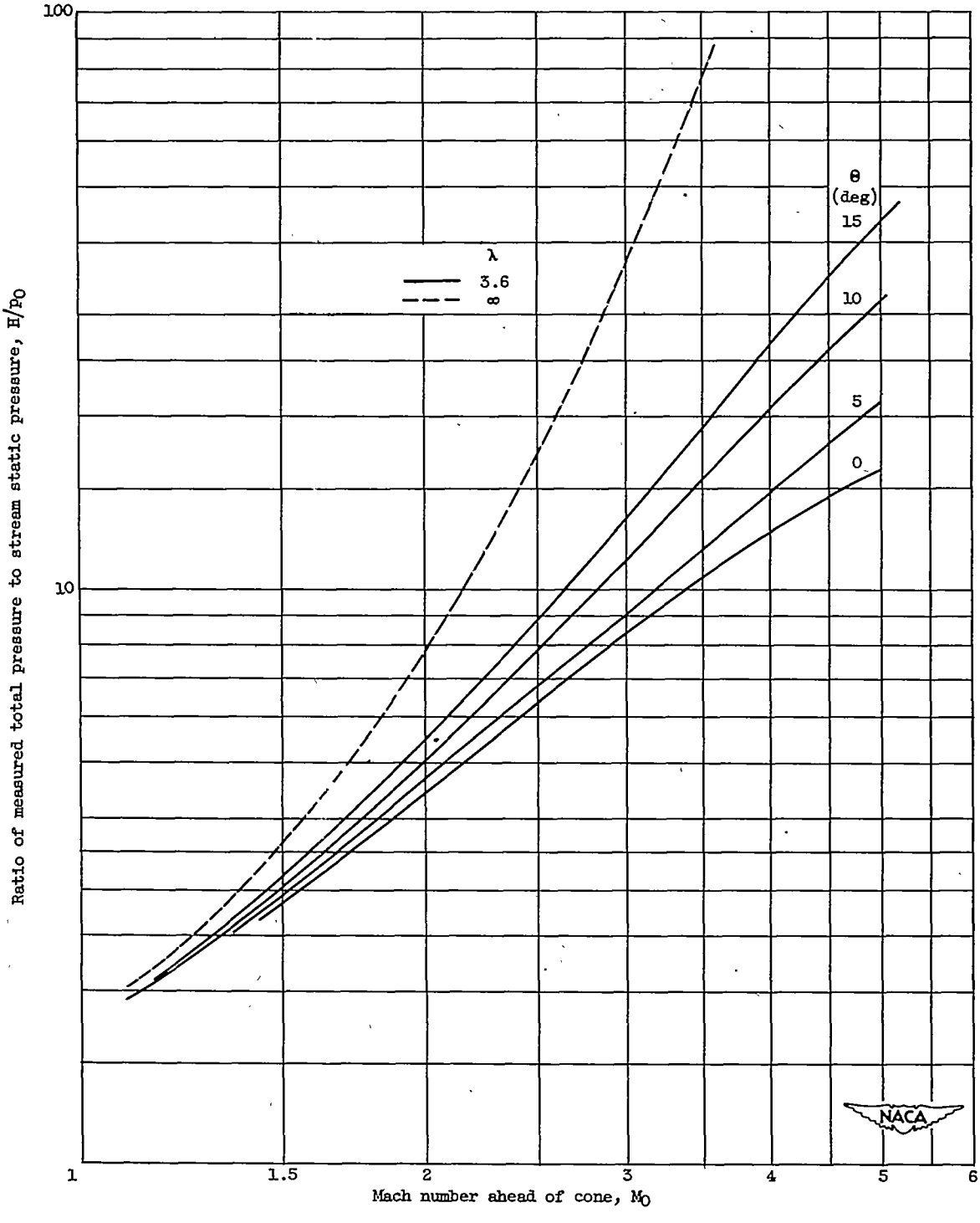

Figure 6. - Expected total pressure at zero angle of attack.

NACA-Langley - 6-10-52 - 1000